Noise-induced chaos in an optically injected semiconductor laser model

S. K. Hwang, J. B. Gao, and J. M. Liu

Department of Electrical Engineering, University of California, Los Angeles, Los Angeles, California 90095-159410
(Received 4 January 1999; revised manuscript received 30 August 1999)

The chaos induced by an intrinsic spontaneous-emission noise in an optically injected semiconductor laser is investigated through a single-mode injection model. A method is developed to quantitatively study the scale-dependent noise effect in general, and the noise-induced chaotic feature in particular. We find that noise at an experimentally measured level can induce chaos in the system. This suggests that noise-induced chaos may indeed exist in real systems. Certain required characteristics for noise to induce chaos are identified: the periodic state itself, when subject to weak noise, should undergo a process that is much more diffusive than the Brownian motion, and the adjacent chaotic states should still behave chaotically on certain finite scales when subject to noise. We believe they are generic features for noise to induce chaos. The correlation dimension of the clean and noisy attractors is also calculated to study noise-induced changes in the geometrical structure of the attractors.

PACS number(s): 42.60.Mi, 42.65.Sf, 42.55.Px

I. INTRODUCTION

Nonlinear dynamics in an optically injected semiconductor laser has recently attracted much attention due to its profound physics and potential applications. The occurrence of instabilities via a period-doubling route to chaos in such a system was numerically predicted by Sacher *et al.* [1], and later experimentally verified by Simpson *et al.* [2]. The dynamics of the system has been experimentally mapped as a function of the injection level and the detuning frequency [3], where two separate chaotic regions were identified. One of the main elements in the dynamics of a semiconductor laser is the intrinsic noise source in the form of spontaneous emission. The effect of this noise source on the locked states of an optically injected semiconductor were investigated in Refs. [4] and [5]. Recently, it was also quantitatively studied how the intrinsic noise affects the oscillatory and chaotic motions of the system [6].

Noise can actually induce a variety of interesting phenomena in nonlinear dynamical systems, such as noise-induced chaos [7–10], noise-induced instabilities [11,12], and noise-induced order [13]. Noise-induced chaos was first found in a forced anharmonic oscillator [7] and later demonstrated in the noisy Logistic map [8] by Crutchfield and co-workers. They suggested [7,8] that periodic states with a high periodicity become unobservable under the influence of noise. Instead, they become bandlike, with the number of bands typically much smaller than their periods. It is these bandlike noisy oscillatory states that are called noise-induced chaotic states. Since a period-doubling cascade is a universal feature of nonlinear dynamical systems, one would expect that chaos associated with this cascade should be readily observed experimentally. To convincingly identify deterministic chaos experimentally, one need to be able to unambiguously distinguish between noise and chaos. This is, however, a difficult issue [14–17]. For example, Osborne and co-workers observed that $1/f^\alpha$ noise generates time series with finite correlation dimensions [14] and converging K_2 entropy estimates [15]. This indicates that one need to more carefully study whether the dynamics of a noise-induced chaoslike attractor is mostly deterministic or mostly stochastic. By re-examining the noisy logistic map [10], we have indeed found that noise-induced chaos does not happen with the main period(2)-doubling cascade in the logistic map. Rather, it occurs at the period-doubling cascades associated with period-3 and period-5 windows. Three features for noise to induce chaos have also been identified.

Since an optically injected semiconductor laser follows the same period-doubling route to chaos as those of the forced anharmonic oscillator and the logistic map, we are inspired to ask whether noise can make transitions from order to chaos in such a system. If noise-induced chaos does occur, are the mechanisms involved similar to those for the noisy logistic map in our previous study [10]? To better study the effect of the noise and the noise-induced chaotic feature, a more quantitative and effective approach will be developed.

The remainder of this paper is outlined as follows. In Sec. II, we describe the coupled equations that characterize the dynamics of an optically injected semiconductor laser. The range of the operating conditions under this study is also presented. In Sec. III, we first consider the test for noise-induced chaos. The time-dependent exponent curve method is then reviewed as the basis in developing a method. A more convenient method is next introduced to study the scale-dependent noise effect in general, and the noise-induced chaotic feature in particular. In Sec. IV, the mechanism for noise to induce chaos is studied. The phase diagrams of attractors and the optical spectra are presented in Sec. V to show how the quantitative results obtained reflects on these more familiar tools. In Sec. VI, we investigate the effect of noise on the geometrical structure of the nonlinear dynamics. Finally, we conclude in Sec. VII.

II. COUPLED EQUATION MODEL

A single-mode model of a semiconductor laser under external optical injection is considered [2]:

$$\frac{da}{dt} = \frac{1}{2}\left[\frac{\gamma_c \gamma_n}{\gamma_s \tilde{J}}\tilde{n} - \gamma_p(2a+a^2)\right]$$

$$\times (1+a) + \xi\gamma_c\cos(\Omega t + \phi) + \mu F_a, \qquad (1)$$

$$\frac{d\phi}{dt} = -\frac{b}{2}\left[\frac{\gamma_c \gamma_n}{\gamma_s \tilde{J}}\tilde{n} - \gamma_p(2a+a^2)\right]$$

$$- \frac{\xi\gamma_c}{1+a}\sin(\Omega t + \phi) + \frac{\mu F_\phi}{1+a}, \qquad (2)$$

$$\frac{d\tilde{n}}{dt} = -\gamma_s\tilde{n} - \gamma_n(1+a)^2\tilde{n} - \gamma_s\tilde{J}(2a+a^2)$$

$$+ \frac{\gamma_s\gamma_p}{\gamma_c}\tilde{J}(2a+a^2)(1+a)^2. \qquad (3)$$

Here $a = (|A|/|A_0| - 1)$, where A is the field amplitude of the injected laser, and A_0 is the steady-state field amplitude of the laser in the free-running condition. ϕ is the phase difference between A and A_i, where A_i is the amplitude of the injection field. $\tilde{n} = (N/N_0 - 1)$, where N is the carrier density of the injected laser and N_0 is the steady-state carrier density of the laser in the free-running condition. γ_c, γ_s, γ_n, and γ_p are the cavity decay rate, the spontaneous carrier relaxation rate, the differential carrier relaxation rate, and the nonlinear carrier relaxation rate, respectively [18]. $\tilde{J} = (J/ed - \gamma_s N_0)/\gamma_s N_0$ is the normalized, dimensionless injection current parameter, where J is the injection current density, e is the electronic charge, and d is the active layer thickness of the laser. The dimensionless injection parameter $\xi = \eta|A_i|/(\gamma_c|A_0|)$ is the normalized strength of the injection field received by the injected laser, where η is the coupling rate of the injection field to the injected laser. $\Omega = \omega_i - \omega_0$ is the frequency detuning of the injection field from the free-running frequency of the injected laser. b is the linewidth enhancement factor. F_a and F_ϕ are the normalized Langevin noise-source parameters that characterize the spontaneous emission in the laser:

$$\langle F_a(t)F_a(t')\rangle = \langle F_\phi(t)F_\phi(t')\rangle = \frac{R_{sp}}{2|A_0|^2}\delta(t-t')$$

$$= \frac{\beta\gamma_c}{2\Gamma\tilde{J}}\delta(t-t'),$$

$$\langle F_a(t)F_\phi(t')\rangle = \langle F_\phi(t)F_a(t')\rangle = 0,$$

where R_{sp} and β are the rate [19] and the fraction of the spontaneous emission into the laser mode, respectively, and Γ is the confinement factor of the laser waveguide. Since the strength of noise can differ by orders of magnitude in different semiconductor lasers, to infer how different noise levels affect the laser dynamics, a coefficient μ is introduced before F_a and F_ϕ. Hence $\mu = 0$ corresponds to an idealized, but unrealistic, clean system in the absence of any noise, while $\mu = 1$ corresponds to the experimentally determined noise level [19] for the laser under consideration.
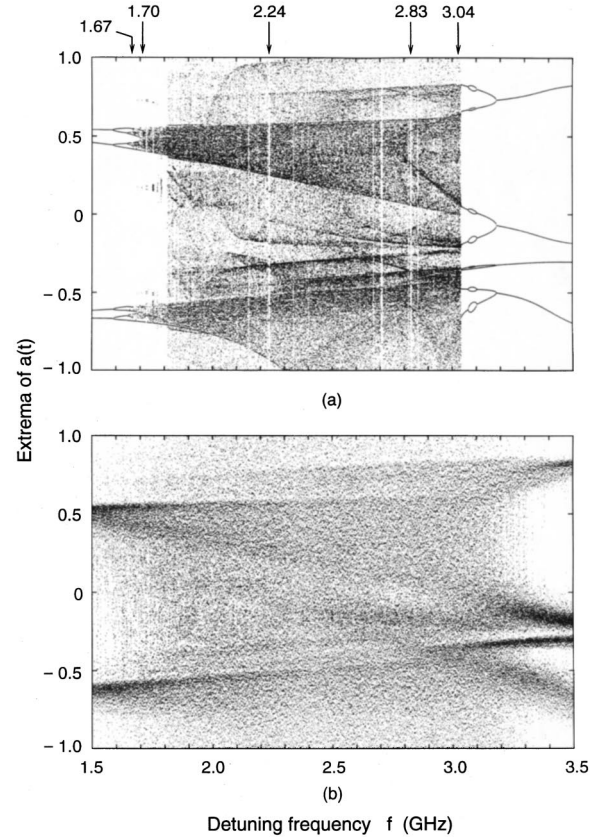

FIG. 1. Numerically obtained bifurcation diagram of the extrema of the normalized optical field amplitude $a(t)$ vs the detuning frequency with (a) $\mu = 0$ and (b) $\mu = 1$. The injection parameter ξ is 0.04.

The laser considered in this investigation is a SDL model 5301-G1 laser diode which is an index-guided GaAs/Al$_x$Ga$_{1-x}$As quantum-well laser with a 500-μm cavity. The current injection level is fixed at $\tilde{J} = 2/3$, which corresponds to an injection current level of 40 mA and a free-running output power of 9 mW. At this current level, the corresponding laser parameters are $\gamma_c = 2.4 \times 10^{11}$ s^{-1}, $\gamma_s = 1.458 \times 10^9$ s^{-1}, $\gamma_n = 1.34 \times 10^9$ s^{-1}, $\gamma_p = 2.41 \times 10^9$ s^{-1}, and $b = 4$. Meanwhile, the relaxation resonance frequency of this laser in the free-running condition is $f_r = 2.93$ GHz. All of these parameters were determined experimentally [18]. The experimentally measured spontaneous emission rate [19] at the operating condition considered here is $R_{sp} = 4.7 \times 10^{18}$ V^2 m^{-2} s^{-1}.

At a given current injection level, the characteristics of an optically injected semiconductor laser depend on the detuning frequency $f = \Omega/2\pi$ and the injection parameter ξ of the injection field. In the present study, the injection parameter is fixed at $\xi = 0.04$, and the detuning frequency is tuned between 1.5 and 3.5 GHz. Figure 1(a) depicts the numerically obtained bifurcation diagram for $\mu = 0$, from which a period-doubling route to chaos is observed. It is found that chaotic states exist in the range extending from below $f = 1.68$ GHz to above $f = 3.03$ GHz. However, there exist periodic windows within this chaotic region, such as those around the detuning frequencies at 1.70, 2.24, and 2.83 GHz. As a comparison, Fig. 1(b) shows the bifurcation diagram for $\mu = 1$. It is observed that the period-doubling cascade is smeared out

by noise. Note that even the periodic states with low periodicity, such as that at the detuning frequency $f=1.5$ GHz, which is a period-2 oscillation, become unobservable under the influence of noise if one were to estimate the periodicity solely on the bifurcation diagram. The question for us is thus whether these apparently aperiodic motions are mostly chaotic, and the period-doubling cascade is mostly inhibited. That is, when noise is present, whether the periodic states still exhibit periodlike motion, similar to that when noise is absent, with some diffusion due to noise, or their dynamical characteristics have completely changed to be more like chaos.

To answer the above question, we choose some of the periodic states at the detuning frequencies $f=1.67$ and 3.04 GHz associated with the main period-doubling cascade, and $f=1.70$, 2.24, and 2.83 GHz in the periodic windows, as shown in Fig. 1, for the following discussions. In addition, to explore how the periodic states and their adjacent chaotic states are related when both are subject to noise, corresponding adjacent chaotic states at $f=1.68$, 1.71, 2.25, 2.84, and 3.03 GHz are also investigated. Note that the chaotic states under present study belongs to one of the two experimentally mapped chaotic regions [3], which is different from the one studied in Ref. [6].

III. TEST FOR NOISE-INDUCED CHAOS

To determine whether noise can induce chaos or not, we need to define chaos carefully. From the mathematical point of view, a noisy system, no matter how weak the noise is, has infinite dimensions. From the experimental point of view, one would, however, be more interested in a certain range of finite scales: if the noise is very weak, then its influence on the dynamics may be limited to very small scales, leaving the dynamics on some finite scales deterministiclike. In the present discussion, this experimental point of view is adopted, and chaos is defined by the exponential divergence between nearby trajectories on certain finite scales. Carefully note the concept of scale in this definition of chaos, since the conventional one based on simply calculating the positive Lyapunov exponent does not take this concept into consideration. Noise-induced chaos is also defined in a similar manner: a certain amount of noise induces exponential divergence between nearby trajectories on certain finite scales in a dynamical system. Since exponential divergence between nearby trajectories is involved, a test for noise-induced chaos has to be able to estimate the largest positive Lyapunov exponent. A suitable test for noise-induced chaos from the proposed algorithms for estimating the positive Lyapunov exponents may be found. These algorithms can be roughly grouped into three types: the well-known algorithm of Wolf *et al.* [20] for estimating the largest positive Lyapunov exponent, a complexity measure proposed by Paladin and co-workers [21,22], which is a weighted version of the largest positive Lyapunov exponent, and a direct dynamical test for deterministic chaos proposed by Gao and Zheng [23]. Before we continue, we need to carefully examine which algorithm can serve as a basis for the study of noise-induced chaos.

To serve as a test for noise-induced chaos, a set of minimal criteria has to be satisfied. The first criterion requires

that different researchers should interpret the obtained results consistently when they apply the test to the same problem. This can be ensured if there is no free parameters to select, or there is a simple, strict procedure for choosing the parameters when using the algorithm. The second criterion, which is as important as the first, is that it will not mislead us to interpret a simple noisy process, such as white noise or a linear Gaussian process, as chaos. These two criteria ensure the notion of determinism in some degree. We will show in the following subsection that among the three algorithms mentioned in the last paragraph, only the method proposed by Gao and Zheng [23] satisfies these two criteria. The test of Gao and Zheng [23] has an additional appealing feature that it has incorporated the notion of scale into the algorithm. Hence it can be used as the basis for the present study without any modification. In Sec. III A we shall first review this method. Meanwhile, we shall point out why the other two algorithms fail to satisfy the above two criteria. We shall then develop a simplified version of Gao and Zheng's method, which will be particularly useful for studying the scale-dependent noise effect with the noise strength fixed.

In order for the analysis presented in this paper to be directly relevant to experimental data analysis, we shall work with scalar time series in the following discussions. Given a scalar time series $x(i)$, $i=1,2,\ldots$, it is now customary to form vectors $X_i=[x(i),x(i+L),\ldots,x(i+(m-1)L)]$ by employing the time delay embedding method [24–26], where L is the delay time and m the embedding dimension. For the analysis of purely chaotic signals, m and L have to be chosen properly. A basic idea to determine the minimum acceptable embedding dimension is that in the passage from dimension m to $m+1$ one can differentiate between points on the orbit $X(n)$ that are true neighbors and points which are false neighbors, points which appear to be neighbors because the orbit is being viewed in too small an embedding space. Based on this basic idea, several methods have been proposed [23,27–30], which differ in implementations either by way of graphic display or by defining some appropriate statistical quantity. Here, we adopt the method proposed by Gao and Zheng [23]. Based on the characteristic of the system, we choose m to be 7 and L to be 5. Since noisy data are infinite dimensional, mathematically speaking, optimal embedding is not defined for the analysis of noisy data. We have found, though, that optimal embedding parameters for a clean chaotic signal are usually also good for the analysis of the corresponding noisy chaotic signal.

A. Time-dependent exponent $\Lambda(k)$ curve

It has been demonstrated [23] that the time series of a nonlinear dynamical system can be conveniently studied by computing the following time-dependent exponent $\Lambda(k)$ curves:

$$\Lambda(k)=\left\langle \ln\left(\frac{\|X_{i+k}-X_{j+k}\|}{\|X_i-X_j\|}\right)\right\rangle, \qquad (4)$$

with $r\leq\|X_i-X_j\|\leq r+\Delta r$, where r and Δr are prescribed small distances. Geometrically $(r,r+\Delta r)$ defines a shell, and a shell captures the notion of scale. The angle brackets denote ensemble averages of all possible pairs of (X_i,X_j).
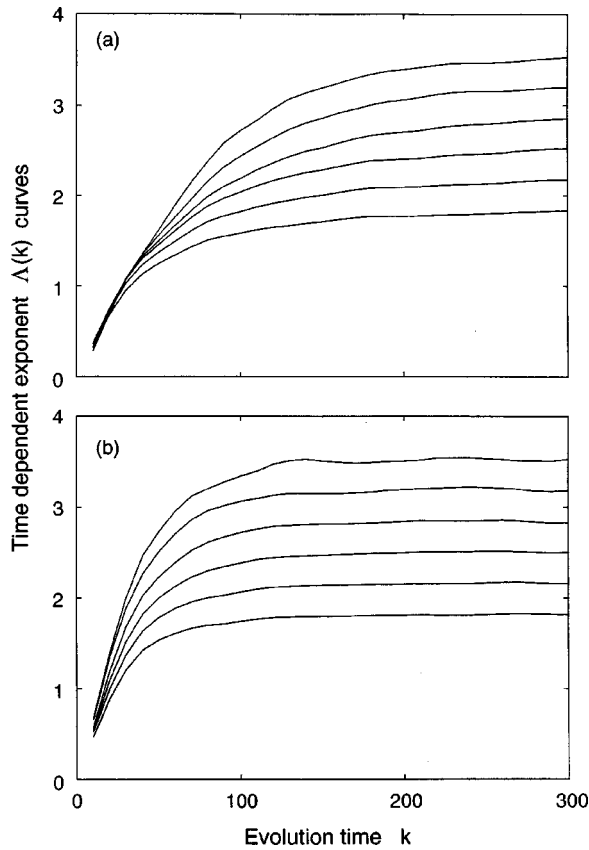
FIG. 2. Time-dependent exponent $\Lambda(k)$ curves as a function of the evolution time k for $f = 2.84$ GHz with (a) $\mu = 0$ and (b) $\mu = 1$. In both plots, six curves, from bottom to top, correspond to shells $(2^{-(i+1)/2}, 2^{-i/2})$ with $i = 6, 7, 8, 9, 10,$ and 11.

The integer k corresponds to the evolution time $k\,\delta t$, and is called the evolution time for simplicity.

For clean chaotic systems, a $\Lambda(k)$ curve typically increases linearly with k until some k_p, then flattens, where k_p is the predictable time scale for chaos. The linearly increasing parts of the $\Lambda(k)$ curves corresponding to different shells overlap together to form an envelope. The slope of this envelope estimates the largest positive Lyapunov exponent. This property provides a direct dynamical test for deterministic chaos [23]. Figure 2(a) shows an example of the $\Lambda(k)$ curves for the chaotic state at $f = 2.84$ GHz, with $\mu = 0$, where six curves, from bottom to top, correspond to shells $(2^{-(i+1)/2}, 2^{-i/2})$ with $i = 6, 7, 8, 9, 10,$ and 11. As for clean periodic systems, $\Lambda(k)$ is simply zero for all k and for all shells, indicating that the largest exponent is zero. This is consistent with a theoretical result of Haken's [31].

For noisy systems, the $\Lambda(k)$ curves corresponding to different shells increase with k and then level off. However, the linearly increasing parts of the $\Lambda(k)$ curves may separate from one another. The stronger the noise is, the more the separation is. An example for the chaotic state at $f = 2.84$ GHz with $\mu = 1$ is shown in Fig. 2(b). Note that the linearly increasing parts of the $\Lambda(k)$ curves for some shells still overlap together, which, according to the definition of chaos, implies that this chaotic state still behaves chaotically at these scales under the influence of noise. For many other chaotic states, such as that at $f = 1.68$ GHz, however, we find that the linearly increasing parts of the $\Lambda(k)$ curves for all

shells separate from one another. This simply suggests that the noisy chaotic motions corresponding to those parameters are more stochastic than deterministic. We have also observed that many noisy oscillatory motions behave similarly as the noisy chaotic motion at $f = 2.84$ GHz.

We can now discuss why in the presence of noise the algorithms of Wolf *et al.* [20] and Paladin and co-workers [21,22] cannot be used as a test for chaos. Their methods are somewhat equivalent to estimating the Lyapunov exponent (or a complexity measure) by $\Lambda(k)/k$, where $\Lambda(k)$ is defined as in Eq. (4) but with a modification: it is computed for $\|X_i - X_j\| < r$ and $\|X_{i+k} - X_{j+k}\| < R$, where r and R are prescribed distance scales. The condition $\|X_i - X_j\| < r$ amounts to grouping some of our small shells together to form a small ball. The condition $\|X_{i+k} - X_{j+k}\| < R$ is presumably to set the time scale k smaller than the prediction time scale k_p. For clean chaotic signals, if the embedding parameters are properly chosen, and the linearly increasing parts of the $\Lambda(k)$ curves form a tight envelope, then an estimation of the exponent will not depend on the specific choice of r and R. However, one is usually not so lucky as to choose those specific optimal embedding parameters. Hence different researchers may obtain different estimates of the exponent by choosing different sets of values for r and R. For example, an inexperienced researcher might unfortunately set k so much larger than k_p that a value of almost zero is obtained for the exponent.

The problem associated with estimating an exponent from a set of stochastic data by using the algorithms of Wolf *et al.* [20] and Paladin and co-workers [21,22] is apparently much more serious than that associated with estimating an exponent from a clean chaotic signal. Since now the $\Lambda(k)$ curves do not form an envelope, different researchers typically will obtain different values for the exponent by choosing different sets of values for r and R (and embedding parameters). One may instinctly choose $k \gg (m-1)L$ such that the estimated exponent may quite often be very close to zero. For a stochastic data set, since the $\Lambda(k)$ curves always increase for $k < (m-1)L$ due to the correlations introduced by the embedding procedure [23], a positive finite value of the exponent can always be obtained for a stochastic data, thus resulting in a false interpretation of the stochastic data being chaotic. Indeed, Dammig and Mitschke [17] found that a finite positive value for the largest positive Lyapunov exponent is obtained from some stochastic data by the algorithm of Wolf *et al.* [20]. The method of Gao and Zheng [23] avoids all these problems because all the important information, such as whether the envelope exists or not, is automatically shown by the $\Lambda(k)$ curves.

The authors of Ref. [8] suggested that the effect of noise is to average the structure of deterministic attractors over some range of nearby parameters, implying that the behavior of adjacent noisy attractors are similar. Therefore, for noise to be able to induce a transition from a periodic state to a chaotic state, the corresponding adjacent chaotic states should still behave chaotically in the presence of such noise. In other words, the adjacent chaotic states should be very insensitive to noise. This suggests that we first study the immunity of chaotic states to noise. Before we proceed, we need to point out that a specific noise source may affect different chaotic states differently: it may have an effect on

the motion of a certain chaotic state only at very small scales, but may affect the motion of other chaotic states at large scales. We call this feature the scale-dependent noise effect. The idea of using a quantity called the normalized area [32] to quantify the effect of noise is not very convenient for studying the scale-dependent noise effect, because the normalized area is calculated based on a specific scale defined by two shells which are somewhat arbitrarily chosen. Therefore, we need to develop a method to quantify scale-dependent noise effect for the comparison of different chaotic states.

B. Scale-dependent Lyapunov exponent

Recall that for clean chaotic systems, the linearly increasing parts of the $\Lambda(k)$ curves corresponding to different shells overlap together to form a linear envelope, and the slope of this envelope estimates the largest positive Lyapunov exponent for the dynamical system. Hence the slope of the linearly increasing part of the $\Lambda(k)$ curve for each shell should be independent of scales (shells) if the envelope is very well defined. We call the slope of the linearly increasing part of the $\Lambda(k)$ curve for each shell the largest positive Lyapunov exponent at that scale, and denote it as $\lambda(r)$ for the shell $(r, r+\Delta r)$, or shell r for simplicity. It is this characteristic that guarantees different researchers to obtain comparable estimates of the largest positive Lyapunov exponent for a dynamical system though each may estimate this value at a different scale. For noisy chaotic systems, the envelope no longer exists, and $\lambda(r)$ generally depends on r. Therefore, the largest positive Lyapunov exponent for noisy chaotic systems is not defined. The extent of the dependence of $\lambda(r)$ on r will, however, tell us how noise affects different scales for different systems. The less dependent on r the $\lambda(r)$ is, the more immune the system is to noise.

Figure 3 shows the value of $\lambda(r)$ for the chaotic states at $f = 1.68$ and 2.84 GHz as a function of $\log r$ for both $\mu = 0$ and $\mu = 1$. It is observed that $\lambda(r)$ has a larger value when noise is present than when noise is absent, indicating that noise increases the degree of exponential divergence between nearby orbits of the chaotic state. It is also observed that the amount of change in the value of $\lambda(r)$ caused by noise at $f = 2.84$ GHz is much smaller than that at $f = 1.68$ GHz. This indicates that the effect of noise on the dynamics at $f = 2.84$ GHz is much less significant than that at $f = 1.68$ GHz.

To be more quantitative, we first denote $\lambda(r)$ of the chaotic state in the presence of noise ($\mu = 1$) as $\lambda_n(r)$ and that in the absence of noise ($\mu = 0$) as $\lambda_c(r)$, and then take their ratio. If the chaotic state is insensitive to noise, then the ratio $\lambda_n(r)/\lambda_c(r)$ should be around 1. Figure 4 shows the ratio $\lambda_n(r)/\lambda_c(r)$ versus $\log_{10} r$ for $f = 1.68$, 1.71, 2.25, 2.84, and 3.03 GHz. They correspond to the chaotic states adjacent to the periodic states at $f = 1.67$, 1.70, 2.24, 2.83, and 3.04 GHz, respectively. Note that the values of the ratio $\lambda_n(r)/\lambda_c(r)$ for $f = 1.68$ and 1.71 GHz decrease with increasing values of $\log_{10} r$ significantly, whereas those for $f = 2.25$, 2.84, and 3.03 GHz only depend weakly on $\log_{10} r$. This indicates that the chaotic states at $f = 2.25$, 2.84, and 3.03 GHz are substantially less sensitive to noise than those at $f = 1.68$ and 1.71 GHz. In other words, when noise is
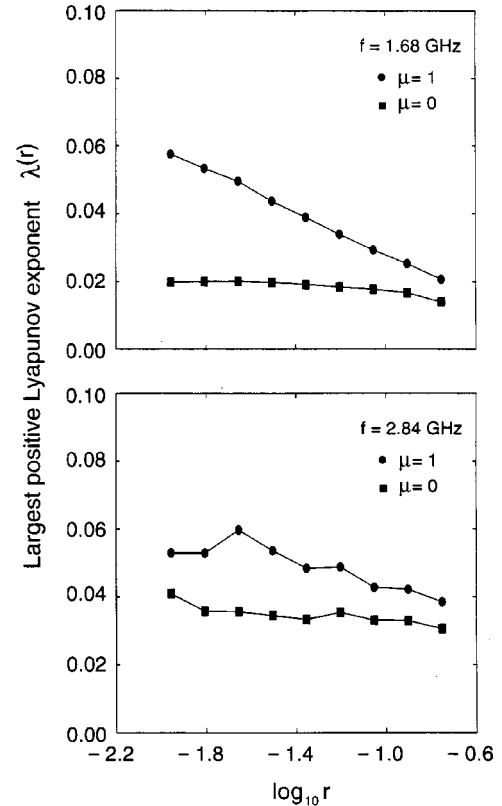

FIG. 3. Slope of the linearly increasing parts of the $\Lambda(k)$ curve, $\lambda(r)$, vs the logarithm of the radius of each shell, $\log_{10} r$, for $f = 1.68$ and 2.84 GHz for the cases of $\mu = 0$ and 1 in both plots.

present, the motions of the chaotic states at $f = 2.25$, 2.84, and 3.03 GHz may still be chaotic on some finite scales, while those at $f = 1.68$ and 1.71 GHz simply become noise-like.

Since the corresponding adjacent chaotic states should be insensitive to noise for periodic states to be susceptible to noise-induced chaos, it is expected from Fig. 4 that noise-induced chaos is very likely to happen around the periodic states at $f = 2.24$, 2.83, and 3.04 GHz, while it is very unlikely to occur around those at $f = 1.67$ and 1.70 GHz. To determine whether noise indeed induces chaos at those expected periodic states, we can simply apply the method just
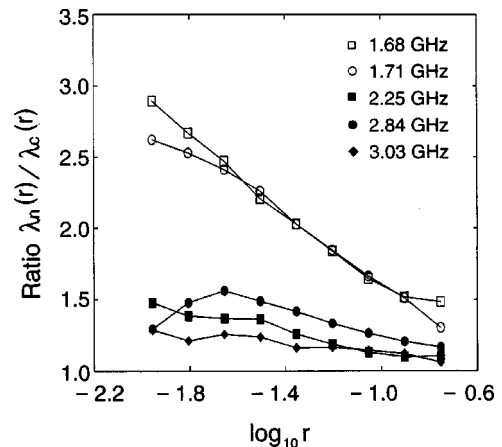

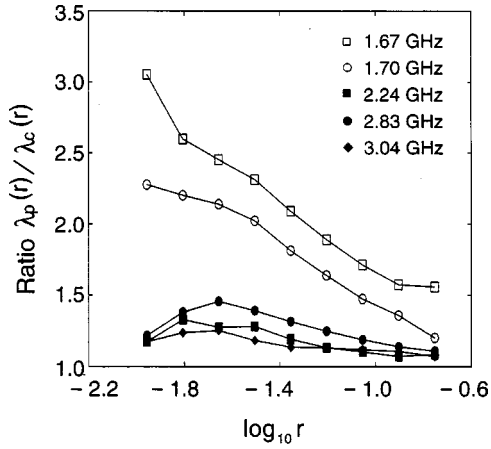FIG. 4. Ratio of λ_n/λ_c vs $\log_{10} r$ for $f = 1.68$, 1.71, 2.25, 2.84, and 3.03 GHz.

FIG. 5. Ratio of λ_p/λ_c vs $\log_{10} r$ for $f = 1.67$, 1.70, 2.24, 2.83, and 3.04 GHz.

FIG. 6. Four logarithmic displacement $\langle \ln\|X_{i+k}-X_{j+k}\| \rangle$ curves, from top to bottom, corresponding to shells $(2^{-(i+1)/2}, 2^{-i/2})$ with $i = 9$, 10, 11, and 12 for (a) $f = 1.67$ GHz and $\mu = 0.007^{1/2}$, (b) $f = 1.70$ GHz and $\mu = 0.003^{1/2}$, (c) $f = 2.24$ GHz and $\mu = 0.000\,009\,3^{1/2}$, (d) $f = 2.83$ GHz and $\mu = 0.0007^{1/2}$, and (e) $f = 3.04$ GHz and $\mu = 0.0007^{1/2}$. Curves generated from $\ln k^{\alpha}$ with $\alpha = 0.4$, 0.35, 0.85, 1.1, and 0.9 are also depicted in (a) as blank squares, (b) diamonds, (c) triangles, (d) circles, and (e) squares, respectively. To aid the visibility, groups of curves (a), (b), (c) and (d) are shifted upward by 10.5, 7.5, 6.0, and 3 units, respectively.

developed to study the dependence of $\lambda(r)$ on r for the periodic states when subject to noise. To study the changes in $\lambda(r)$ caused by the presence of noise for a periodic state, it is instructive to compare its noisy motion with the clean motion of its adjacent chaotic state because adjacent dynamical states are suggested [8] to behave similarly when subject to noise. Therefore, we first calculate $\lambda(r)$ for the periodic state in the presence of noise, denote it as $\lambda_p(r)$, and calculate $\lambda(r)$ for its adjacent chaotic state in the absence of noise, denote it as $\lambda_c(r)$. We then take their ratio. The ratio $\lambda_p(r)/\lambda_c(r)$ is expected to be around 1 if noise-induced chaos happens. Figure 5 shows the ratio $\lambda_p(r)/\lambda_c(r)$ as a function of $\log_{10} r$ for the periodic states at $f = 1.67$, 1.70, 2.83, 2.24, and 3.04 GHz. It can be concluded from Fig. 5 that noise-induced chaos does occur at $f = 2.24$, 2.83, and 3.04 GHz, but it does not occur at $f = 1.67$ and 1.70 GHz. Moreover, if we compare Fig. 5 with Fig. 4 carefully, we find that the periodic state and its adjacent chaotic state do behave similarly when both are subject to noise, as suggested in Ref. [8].

IV. MECHANISM FOR NOISE-INDUCED CHAOS

To find the mechanism for noise-induced chaos, we need to work with the so-called logarithmic displacement curves, and examine the long-term growth rate of these curves when subject to weak noise. The logarithmic displacement curves are defined by rewriting Eq. (4) as [32]

$$\langle \ln\|X_{i+k}-X_{j+k}\| \rangle = \langle \ln\|X_i-X_j\| \rangle + \Lambda(k), \qquad (5)$$

and plot $\langle \ln\|X_{i+k}-X_{j+k}\| \rangle$ as a function of the evolution time k.

It has been demonstrated [32] that for noisy oscillatory systems, such as the noisy Van der Pol's oscillator, the phase points in the embedding space execute Brownian-like motion near a deterministic limit cycle, i.e., for large k, $\langle \ln\|X_{i+k}-X_{j+k}\| \rangle \sim \ln k^{\alpha}$, with $\alpha = 0.5$. It has also been shown that the long-term growth rate of the logarithmic displacement curves slows down near a bifurcation point in an optically injected semiconductor laser [6], which is characterized by an exponent $\alpha < 0.5$. This implies a diffusional process slower than the standard Brownian motion. More interestingly, it has
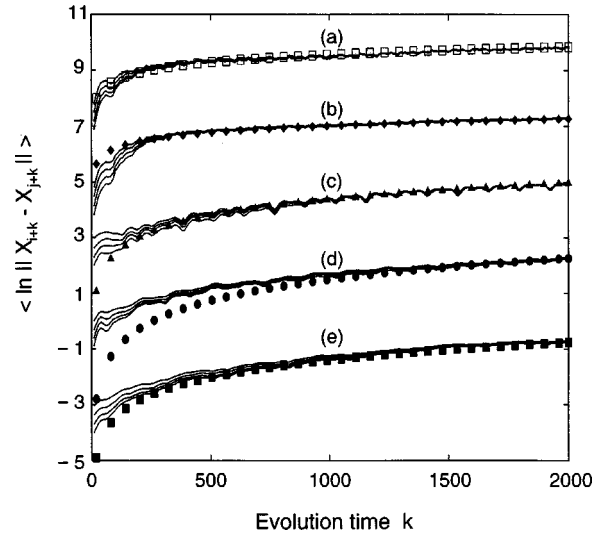
been shown in the noisy logistic map [10] that, for noise of a certain strength to induce chaos from a periodic state, the long-term growth rate of the logarithmic displacement curves for this periodic state when subject to noise of a weaker strength is stronger than the standard Brownian motion, characterized by an exponent $\alpha > 0.5$.

With the above results in mind, we study the behavior of the logarithmic displacement curves for the periodic states subject to noise of a weak strength ($\mu < 1$). These are shown in Fig. 6 for (a) $f = 1.67$ GHz with $\mu = 0.007^{1/2}$, (b) $f = 1.70$ GHz with $\mu = 0.003^{1/2}$, (c) $f = 2.24$ GHz with $\mu = 0.000\,009\,3^{1/2}$, (d) $f = 2.83$ GHz with $\mu = 0.0007^{1/2}$, and (e) $f = 3.04$ GHz with $\mu = 0.0007^{1/2}$. To aid the visibility, these groups of curves are shifted upward by different amounts. To show the growth rate of the logarithmic displacement curves, curves generated from $\ln k^{\alpha}$ with $\alpha = 0.4$, 0.35, 0.85, 1.1, and 0.9 for $f = 1.67$, 1.70, 2.24, 2.83, and 3.04 GHz, respectively, are also depicted. Diffusional processes that are slower than the standard Brownian motion are observed at $f = 1.67$ and 1.70 GHz, where a transition from periodic states to chaos does not occur. The growth rates of the logarithmic displacement curves for $f = 2.24$, 2.83, and 3.04 GHz are larger than 0.5, indicating diffusional processes stronger than the standard Brownian motion.

Note that when noise-induced chaos occurs, the noisy system with certain amount of noise exhibits an exponential growth in the displacement curves for a short period of time, then levels off. Such behavior is easier to observe if the noisy system with a weaker noise already executes a diffusional process stronger than the Brownian motion. This is the reason why noise is able to induce chaos at $f = 2.24$, 2.83, and 3.04 GHz, but is not capable of doing so at $f = 1.67$ and 1.70 GHz, for the diffusional processes of the latter are
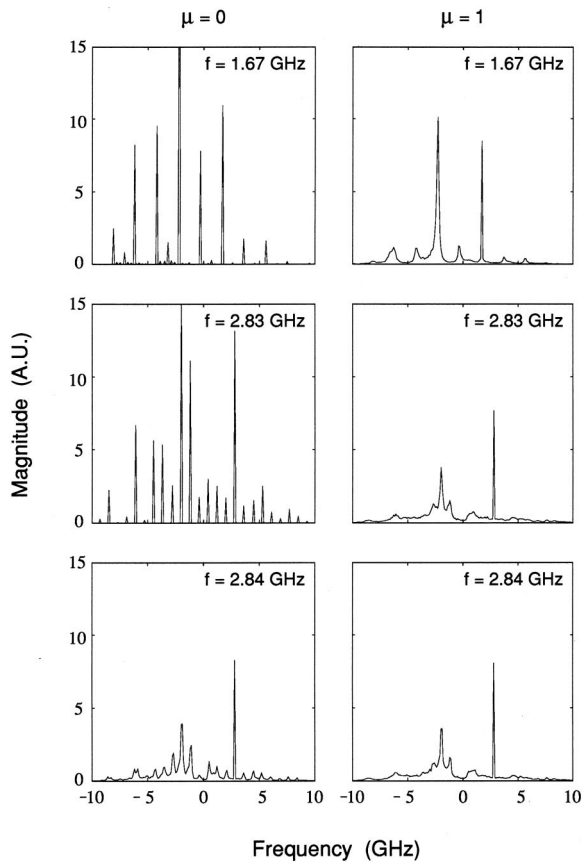
FIG. 7. Optical spectra for $f = 1.67$, 2.83, and 2.84 GHz for the cases of $\mu = 0$ and 1.

FIG. 8. Projections of three-dimensional attractors on two dimensions for $f = 1.67$, 2.83, and 2.84 GHz for the cases of $\mu = 0$ and 1.

slower than the standard Brownian motion. Note that this very condition is also involved in the periodic states susceptible to noise-induced chaos in the noisy logistic map [10]. We surmise that this is a generic mechanism for noise to induce chaos, and thus has predictive value.

V. PHASE DIAGRAM AND OPTICAL SPECTRUM

Let us now look at the dynamics of our clean and noisy systems with the more familiar tools: phase diagrams and optical spectra. To be simple, only a few of the dynamical states will be discussed. However, the results presented apply to other corresponding cases.

Figure 7 shows the optical spectra of the system in different operating conditions. The optical spectrum is an important and common tool in laser physics and engineering because it exhibits all frequency components of an optical field, which thus reflects certain aspects of the dynamics of the system. It is found that when noise is absent, the optical spectra at $f = 1.67$ and 2.83 GHz consist of discrete, relatively narrow peaks that are regularly spaced, which are the signature of periodic oscillation for this system [2,3]. In comparison, the spectrum at $f = 2.84$ GHz is dominated by a broad pedestal with some strong secondary peaks, revealing the chaotic characteristic of the system [2,3]. These observations also reflect on the structure of corresponding attractors shown in Fig. 8.

Also shown in Fig. 7 is the spectrum of the system subject to noise. For the periodic state at $f = 1.67$ GHz, although the
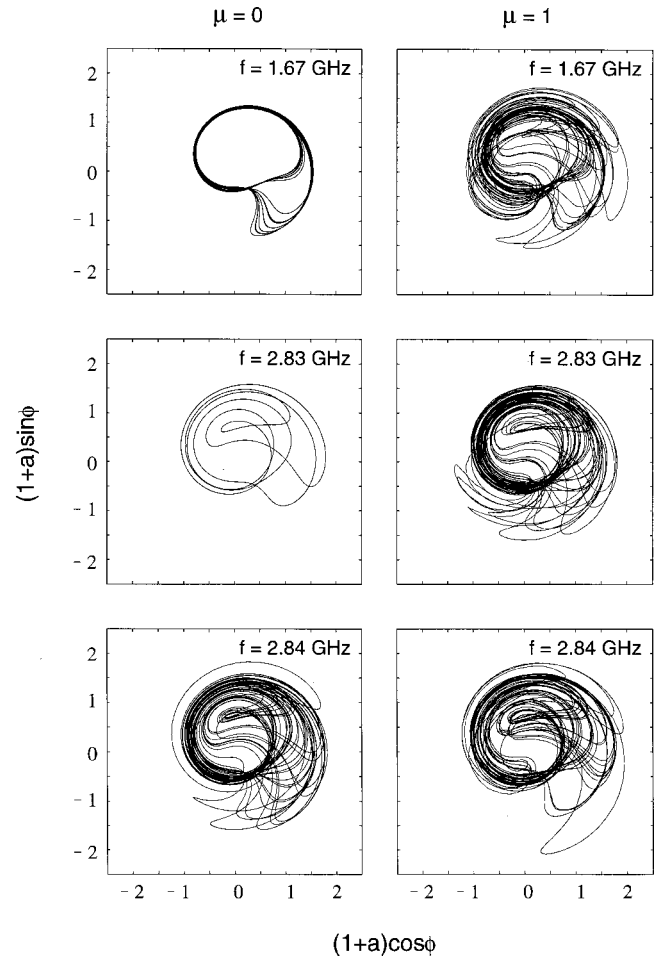
spectrum shows some broadening around each principal frequency, many of the principal frequencies still remain as peaks. This suggests that the system still oscillates periodically but the periodic motion is obscured by noise to a certain degree. In contrast, for the periodic state at $f = 2.83$ GHz, the spectrum is dominated by broad pedestals, and only a few of the principal frequencies remain as peaks, indicating the loss of the periodic characteristic. This observation is consistent with our earlier conclusion that noise induces chaos at $f = 2.83$ GHz but not at $f = 1.67$ GHz. Note, however, that the difference between these two noisy states is difficult to distinguish by solely observing the corresponding attractors in Fig. 8.

For the chaotic state at $f = 2.84$ GHz, we find that the spectrum preserves most of features with and without noise. This suggests that the chaotic state at $f = 2.84$ GHz still behaves chaotically when noise is present. The same result may also be observed from Fig. 8, where the chaotic attractor subject to noise is only blurred in small scales but is preserved in large scales. On the other hand, we find that under the influence of noise, the spectrum and attractor for the chaotic state at $f = 1.68$ GHz become completely different, indicating a noiselike characteristic of the dynamics. These observations are consistent with the quantitative result obtained earlier and shown in Fig. 4, that the effect of noise on

the chaotic dynamics at $f = 1.68$ GHz is substantially stronger than that at $f = 2.84$ GHz. It is also found that when noise is present, the spectra for $f = 2.83$ and 2.84 GHz are very similar to each other. This is in agreement with the earlier observation that a periodic state and its adjacent chaotic state behave similarly. This is also reflected in the similarity of the noisy attractors between $f = 2.83$ and 2.84 GHz, as shown in Fig. 8. These observations in geometrical structure of attractors, shown in Fig. 8, suggest that we calculate the correlation dimensions [33,34] of the chaotic states and the noise-induced chaotic states.

VI. CORRELATION DIMENSION OF NOISE-INDUCED CHAOTIC STATES

The correlation integral $C(N,r)$ of a dynamical state is defined as [33]

$$C(N,r) = \frac{1}{N^2} \sum_{i,j=1}^{N} \theta(r - \|X_i - X_j\|), \qquad (6)$$

where θ is the Heaviside step function, X_i and X_j are the vectors constructed from the time series, N is the number of points in the time series, and r is a prescribed small distance. The correlation dimension of the dynamical state is then given by

$$\nu = \lim_{r \to 0} \lim_{N \to \infty} \frac{\log_{10} C(N,r)}{\log_{10} r}. \qquad (7)$$

Here we measure the local slope of the correlation integral $\log_{10} C(N,r)$ instead for different values of the small distance r by calculating

$$\nu(r_i) = \frac{\log_{10} C(N,r_{i-1}) - \log_{10} C(N,r_{i+1})}{\log_{10} r_{i-1} - \log_{10} r_{i+1}}. \qquad (8)$$

Figure 9 shows the values of the local slope of the correlation integral $\log_{10} C(N,r)$ as a function of $\log_{10} r$ for $f = 1.68$ and 2.84 GHz, respectively. For $f = 1.68$ GHz, we find that the curves of the local slope for $\mu = 0$ and $\mu = 1$ are separated at all scales, indicating that noise completely destroys the original structure of the clean attractor. In contrast, it is found that for $f = 2.84$ GHz, the local slopes of the correlation integral with $\mu = 0$ and 1 overlap at some large scales but separate at small scales. This indicates that some fine structures of the attractor are destroyed by noise, but the entire noisy attractor is left chaoslike with the general characteristics of the clean chaotic attractor. Note that noise-induced chaos occurs at $f = 2.84$ GHz, not at $f = 1.68$ GHz. These results indicate that, in the presence of noise, a chaotic state adjacent to a periodic state where noise-induced chaos happens preserves approximately the same geometrical structure, whereas that adjacent to a periodic state where noise-induced chaos is not observed exhibits a completely different geometrical structure. This alternatively tells us that noise does have much less effect on the dynamics of a chaotic state adjacent to a periodic state where noise-induced chaos happens.

Also shown in Fig. 9 are the values of the local slope of the correlation integral $\log_{10} C(N,r)$ for the periodic states at
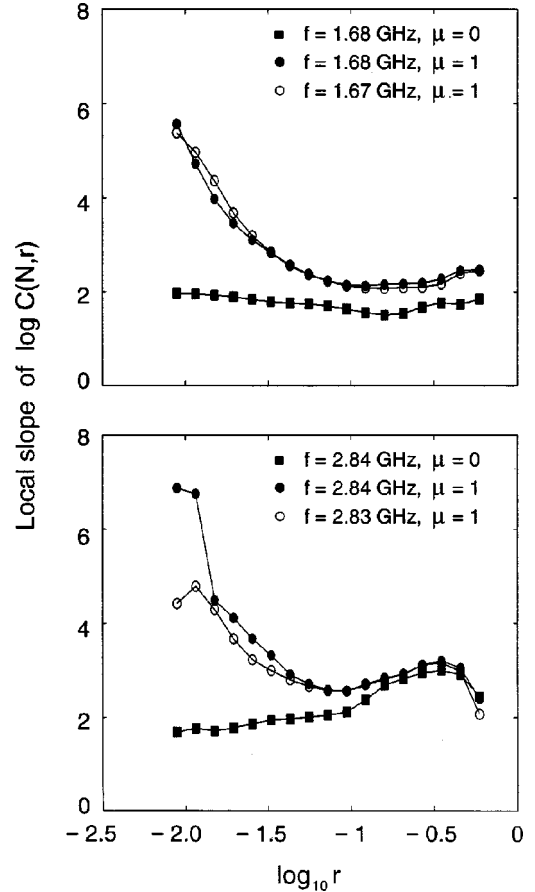

FIG. 9. Local slope of the correlation integral $\log_{10} C(N,r)$ vs $\log_{10} r$ for $f = 1.68$ and 2.84 GHz for the cases of $\mu = 0$ and 1. Also shown are $f = 1.67$ and 2.83 GHz for $\mu = 1$.

$f = 1.67$ and 2.83 GHz, with $\mu = 1$. We observe that in the presence of noise, the curves of the local slope for $f = 1.67$ and 2.83 GHz behave approximately the same way as those for their corresponding adjacent chaotic states at $f = 1.68$ and 2.84 GHz. This tells us that when subject to noise, a periodic state and its adjacent chaotic state have similar geometrical structures. Moreover, it indicates that a noise-induced chaotic state does share a similar geometrical structure as its adjacent chaotic state in the presence of noise.

VII. CONCLUSION

The effect of the intrinsic spontaneous-emission noise on the nonlinear dynamics of an optically injected semiconductor laser is investigated to find whether noise with an experimentally determined level can induce chaos in such a system. To study the observed noise effects, we develop a method by studying the dependence of the largest positive Lyapunov exponent on scales for noisy systems. This method is shown to provide a quantitative and effective approach to the study of the scale-dependent noise effect and the characteristics of noise-induced chaos. By employing this method, we find that a chaotic state adjacent to a periodic state where noise-induced chaos is expected to happen is insensitive to noise, leaving the chaotic state still chaoslike in the presence of noise. Most importantly, we find that noise-induced chaos does occur at the periodic states as ex-

pected. Because the laser model used here was shown [2,3] to successfully recover all the oscillatory and chaotic states of the system observed experimentally, this result implies that noise with an experimentally determined strength does induce chaos in the system under certain operating conditions, suggesting that noise-induced chaos indeed exists in real systems. The key reason for noise to induce chaos is that the periodic state should execute a diffusional process stronger than the standard Brownian motion when subject to noise of a weak strength. It is this condition that allows noise, when its strength is increased, to easily induce exponential divergence between nearby orbits, which is a characteristic of deterministic chaos. Note that this characteristic of the periodic state together with the characteristic that its adjacent chaotic state is insensitive to noise are also involved in the noisy logistic map [10] for noise-induced chaos to happen. This implies that these two characteristics are generic features for noise to induce chaos.

To study the effect of noise on the geometrical structure of the dynamical states, the correlation dimensions of the attractors are calculated. It is found from this study that, when subject to noise, a chaotic state adjacent to a periodic state where noise-induced chaos happens preserves most of its original geometrical structure in large scales, whereas the geometrical structure of a chaotic state adjacent to a periodic state where noise-induced chaos is not observed is completely changed in the presence of noise. Moreover, we also find that a noise-induced chaotic state shares a similar geometrical structure with its adjacent chaotic state in the presence of noise.

[1] J. Sacher, D. Baums, P. Panknin, W. Elsasser, and E. O. Gobel, Phys. Rev. A **45**, 1893 (1992).

[2] T. B. Simpson, J. M. Liu, A. Gavrielides, V. Kovanis, and P. M. Alsing, Appl. Phys. Lett. **64**, 3539 (1994); Phys. Rev. A **51**, 4181 (1995).

[3] V. Kovanis, A. Gavrielides, T. B. Simpson, and J. M. Liu, Appl. Phys. Lett. **67**, 2780 (1995).

[4] P. Spano, S. Piazzolla, and M. Tamburrini, IEEE J. Quantum Electron. **22**, 427 (1986).

[5] M. R. Surette, D. R. Hjelme, and A. R. Mickelson, IEEE J. Quantum Electron. **29**, 1046 (1993).

[6] J. B. Gao, S. K. Hwang, and J. M. Liu, Phys. Rev. A **59**, 1582 (1999).

[7] J. P. Crutchfield and B. A. Huberman, Phys. Lett. A **77A**, 407 (1980).

[8] J. P. Crutchfield, J. D. Farmer, and B. A. Huberman, Phys. Rep. **92**, 45 (1982).

[9] R. L. Kautz, J. Appl. Phys. **58**, 424 (1985).

[10] J. B. Gao, S. K. Hwang, and J. M. Liu, Phys. Rev. Lett. **82**, 1132 (1999).

[11] A. R. Bulsara, E. W. Jacobs, and W. C. Schieve, Mod. Phys. Lett. A **42**, 4614 (1990).

[12] Z. Y. Chen, Mod. Phys. Lett. A **42**, 5837 (1990).

[13] K. Matsumoto and I. Tsuda, J. Stat. Phys. **31**, 87 (1983).

[14] A. R. Osborne and A. Provenzale, Physica D **35**, 357 (1989).

[15] A. R. Osborne, A. Provenzale, and R. Soj, Physica D **47**, 361 (1991).

[16] J. Theiler, S. Eubank, A. Longtin, and B. Galdrikian, Physica D **58**, 77 (1992).

[17] M. Dammig and F. Mitschke, Phys. Lett. A **178**, 385 (1993).

[18] J. M. Liu and T. B. Simpson, IEEE J. Quantum Electron. **30**, 957 (1994); IEEE Photonics Technol. Lett. **4**, 380 (1993).

[19] T. B. Simpson and J. M. Liu, Opt. Commun. **112**, 43 (1994).

[20] A. Wolf, J. B. Swift, H. L. Swinney, and J. A. Vastano, Physica D **16**, 285 (1985).

[21] G. Paladin, M. Serva, and A. Vulpiani, Phys. Rev. Lett. **74**, 66 (1995).

[22] V. Loreto, G. Paladin, and A. Vulpiani, Phys. Rev. E **53**, 2087 (1996).

[23] J. B. Gao and Z. M. Zheng, Phys. Lett. A **181**, 153 (1993); Europhys. Lett. **25**, 485 (1994); Phys. Rev. E **49**, 3807 (1994).

[24] N. H. Packard, J. D. Crutchfield, J. D. Farmer, and R. S. Shaw, Phys. Rev. Lett. **45**, 712 (1980).

[25] F. Takens, in *Dynamical Systems and Turbulence*, edited by D. A. Rand and L. S. Young, Lecture Notes in Mathematics Vol. 898 (Springer-Verlag, Berlin, 1981), p. 366.

[26] T. Sauer, J. A. Yorke, and M. Casdagli, J. Stat. Phys. **65**, 579 (1991).

[27] A. Cenys and K. Pyragus, Phys. Lett. A **129**, 227 (1988).

[28] Z. Aleksic, Physica D **52**, 362 (1991).

[29] W. Liebert, K. Pawelzik, and H. G. Schuster, Europhys. Lett. **14**, 521 (1991).

[30] M. B. Kennel, R. Brown, and H. D. I. Abarbanel, Phys. Rev. A **45**, 3403 (1992).

[31] H. Haken, Phys. Lett. **94A**, 71 (1983).

[32] J. B. Gao, Physica D **106**, 49 (1997).

[33] P. Grassberger and I. Procaccia, Phys. Rev. Lett. **50**, 346 (1983).

[34] J. Theiler, J. Opt. Soc. Am. A **7**, 1055 (1990).